Defective lysosome maturation and Legionella pneumophila replication in Dictyostelium cells mutant for the Arf GAP ACAP-A

Nathalie Baïlo, Pierre Cosson, Steve J. Charette, Valérie E. Paquet, Patricia Doublet, François Letourneur

© 2014. Published by The Company of Biologists Ltd | Journal of Cell Science (2014) 127, 4702–4713 doi:10.1242/jcs.154559

RESEARCH ARTICLE

Defective lysosome maturation and *Legionella pneumophila* replication in *Dictyostelium* cells mutant for the Arf GAP ACAP-A

Nathalie Baïlo[1,2,3,4,5], Pierre Cosson[6], Steve J. Charette[7,8,9], Valérie E. Paquet[7,8,9], Patricia Doublet[1,2,3,4,5] and François Letourneur[10,*]

ABSTRACT

Dictyostelium discoideum ACAP-A is an Arf GTPase-activating protein (GAP) involved in cytokinesis, cell migration and actin cytoskeleton dynamics. In mammalian cells, ACAP family members regulate endocytic protein trafficking. Here, we explored the function of ACAP-A in the endocytic pathway of *D. discoideum*. In the absence of ACAP-A, the efficiency of fusion between post-lysosomes and the plasma membrane was reduced, resulting in the accumulation of post-lysosomes. Moreover, internalized fluid-phase markers showed extended intracellular transit times, and the transfer kinetics of phagocyted particles from lysosomes to post-lysosomes was reduced. Neutralization of lysosomal pH, one essential step in lysosome maturation, was also delayed. Whereas expression of ACAP-A–GFP in *acapA*$^{-}$ cells restored normal particle transport kinetics, a mutant ACAP-A protein with no GAP activity towards the small GTPase ArfA failed to complement this defect. Taken together, these data support a role for ACAP-A in maturation of lysosomes into post-lysosomes through an ArfA-dependent mechanism. In addition, we reveal that ACAP-A is required for efficient intracellular growth of *Legionella pneumophila*, a pathogen known to subvert the endocytic host cell machinery for replication. This further emphasizes the role of ACAP-A in the endocytic pathway.

KEY WORDS: Arf GAP, *D. discoideum*, Membrane trafficking, Lysosome, Host-pathogen interaction, *Legionella pneumophila*

INTRODUCTION

The amoeba *Dictyostelium discoideum* is a genetically tractable model organism extensively used to study membrane trafficking in the endocytic pathway. In this professional phagocyte, engulfed material travels through a series of internal compartments (Maniak, 2003). Rapidly after uptake, newly formed macropinosomes and phagosomes recruit the vacuolar proton ATPase (H^+-ATPase) and hydrolytic enzymes to form acidic lysosomes. About 30 min later, lysosomes mature into neutral post-lysosomes, and finally undigested material is ejected from the cells by exocytosis. One key step in lysosome maturation is the depletion of H^+-ATPase from lysosomes leading to pH neutralization. H^+-ATPase retrieval is mediated by small actin-coated vesicles budding from lysosomes (Carnell et al., 2011; Clarke et al., 2010). The role of actin is essential in this process. Hence, depolymerization of F-actin by drugs or the absence of Wiskott–Aldrich syndrome protein (WASH) or Scar family proteins, actin nucleation-promoting factors recruited on these recycling vesicles, completely blocks H^+-ATPase retrieval and lysosome maturation (Carnell et al., 2011; King et al., 2013).

In mammalian cells, the ADP-ribosylation factors (Arfs) proteins regulate endosomal membrane traffic by cycling between active GTP-bound and inactive GDP-bound forms (D'Souza-Schorey and Chavrier, 2006; Donaldson and Jackson, 2011; Gillingham and Munro, 2007). Arf activity is regulated by Arf guanine-nucleotide-exchange factors (Arf GEFs) and by Arf GTPase-activating proteins (Arf GAPs) that promote hydrolysis of GTP bound to Arf. Among the Arf GAP family of proteins, the ACAP subfamily includes three members (ACAP1–ACAP3) in mammalian cells, and comprises four functional domains: a Bin, amphiphysin and Rvs (BAR) domain, a pleckstrin homology (PH) domain, a GAP domain and an ankyrin repeat (ANK) domain. ACAPs mainly regulate the dynamic reorganization of the actin cytoskeleton (Inoue and Randazzo, 2007; Kobayashi and Fukuda, 2012; Kobayashi and Fukuda, 2013; Randazzo et al., 2007), although functions in cargo recycling from endosomes have been reported (Li et al., 2005a; Li et al., 2007). *D. discoideum* has only one Arf protein (ArfA), which is a substrate for the two members of the ACAP subfamily (ACAP-A and ACAP-B) in this amoeba (Chen et al., 2010; Gillingham and Munro, 2007; Weeks, 2005). We have recently shown that ACAP-A is specifically involved in cytokinesis, cell migration and actin cytoskeleton dynamics in an ArfA-dependent manner (Dias et al., 2013). However, the role of ACAPs in the endocytic pathway of *D. discoideum* is still unknown.

Legionella pneumophila is the causative agent of Legionnaires' disease and leads to acute pneumonia in humans after inhalation of contaminated water aerosols (Lamoth and Greub, 2010). *L. pneumophila* pathogenic strains emerge after intracellular multiplication in protozoans and then infect human lung alveolar macrophages. *L. pneumophila* has developed a strategy to escape host-cell defenses mainly by altering membrane trafficking mechanisms in the endocytic and secretory pathways. Upon injection of effector proteins by a bacterial

[1]CIRI, International Centre for Infectiology Research, Legionella pathogenesis group, Université de Lyon, 69364 Lyon Cedex 07, France. [2]Inserm, U1111, 69342 Lyon Cedex 07, France. [3]Ecole Normale Supérieure de Lyon, 69007 Lyon, France. [4]Université Lyon 1, Centre International de Recherche en Infectiologie, 69364 Lyon Cedex 07, France. [5]CNRS, UMR5308, 69007 Lyon, France. [6]Département de Physiologie Cellulaire et Métabolisme, Centre Médical Universitaire, 1 rue Michel Servet, 1211 Geneva 4, Switzerland. [7]Institut de Biologie Intégrative et des Systèmes, Université Laval, Québec, QC G1V 0A6, Canada. [8]Département de Biochimie, de Microbiologie et de Bio-informatique, Université Laval, Québec, G1V 0A6, Canada. [9]Centre de Recherche de L'institut Universitaire de Cardiologie et de Pneumologie de Québec, Québec, QC G1V 4G5, Canada. [10]Laboratoire de Dynamique des Interactions Membranaires Normales et Pathologiques, Universités de Montpellier II et I, CNRS, UMR 5235, Place Eugène Bataillon, 34095 Montpellier Cedex 05, France.

*Author for correspondence (francois.letourneur@univ-montp2.fr)

Received 3 April 2014; Accepted 22 August 2014

Journal of Cell Science

Journal of Cell Science (2014) 127, 4702–4713 doi:10.1242/jcs.154559

type IV secretion system, *L. pneumophila* drives the formation of an intracellular compartment, the '*Legionella*-containing vacuole' (LCV), and avoids the normal host cell endocytic pathway (Allombert et al., 2013; Xu and Luo, 2013). Insights into *L. pneumophila* virulence have been advantageously provided by studies using *D. discoideum* as a host cell model because *L. pneumophila* can infect this amoeba with features highly comparable to that observed in human macrophages (Hägele et al., 2000; Solomon et al., 2000). Hence, newly formed LCVs are transported inside the cell on microtubules and rapidly acquire endoplasmic reticulum (ER) markers. Concomitantly, a reduced fusion rate with lysosomes results in a low amount of vacuolar H^+-ATPase in these endomembrane structures (Lu and Clarke, 2005). Interestingly, the GTPase Arf1 has been shown to participate in the biogenesis of the LCV in macrophages (Derré and Isberg, 2004; Kagan and Roy, 2002; Kagan et al., 2004) and the *L. pneumophila* effector protein RalF has been described to recruit and activate Arf1 to the LCV (Nagai et al., 2002). Although ArfA is known to be present in newly formed LCVs (Urwyler et al., 2009), it is unknown whether ArfA plays a similar role to Arf1 in *D. discoideum* infected cells.

In this study, we explored the function of ACAP-A in the endocytic pathway. We report for the first time that ACAP-A, but not ACAP-B, is involved in maturation of lysosomes, through an Arf-dependent mechanism, and in fusion of post-lysosomes with the plasma membrane. Moreover, we show that ACAP-A is specifically required for the efficient intracellular growth of *Legionella pneumophila*, revealing thus an unexpected role of this Arf GAP in host-defense mechanisms against pathogens.

RESULTS

Fluid-phase endocytic defects in the absence of ACAP-A

The role of ACAP-A in the formation of actin filopodia (Dias et al., 2013) prompted us to assess whether this Arf GAP is involved in fluid-phase and particle endocytosis, two other actin-driven processes. To evaluate the role of ACAP-A in fluid-phase endocytosis, cells in which the gene encoding ACAP-A has been disrupted (*acapA*$^-$ cells) (Dias et al., 2013) were incubated with the fluid-phase marker Alexa-Fluor-647-labeled dextran, and uptake was monitored by flow cytometry (Fig. 1A). *acapA*$^-$ and wild-type (WT) cells showed comparable rates of uptake for the first 20 min. However, whereas uptake began to plateau after 60 min in WT cells, uptake continued to rise in *acapA*$^-$ cells (180.6% of WT uptake after 160 min). When *acapA*$^-$ cells were stably transfected with GFP-tagged ACAP-A, fluid-phase uptake markers did not accumulate anymore and uptake was even slightly inhibited (Fig. 1A). Dextran accumulation in *acapA*$^-$ cells suggested that the extracellular release of the fluid-phase marker might be defective in these cells. Alternatively, a prolonged intracellular transit time of dextran might also delay fluid-phase discharge in *acapA*$^-$ cells. To discriminate between these two possibilities, we first measured fluid-phase exocytosis in *acapA*$^-$ cells. Cells were loaded overnight with Alexa-Fluor-647–dextran, washed in dextran-free medium, and the fluorescence remaining in cells over time was measured. Similar rates of exocytosis were observed in *acapA*$^-$ and WT cells for the first 40 min (Fig. 1B), indicating normal egress of post-lysosomes in the absence of ACAP-A. However, analysis of later time points revealed that there was a slight reduction in exocytosis kinetics in *acapA*$^-$ cells. Next, the intracellular transit time of fluid-phase was determined. Cells were pulsed for 10 min

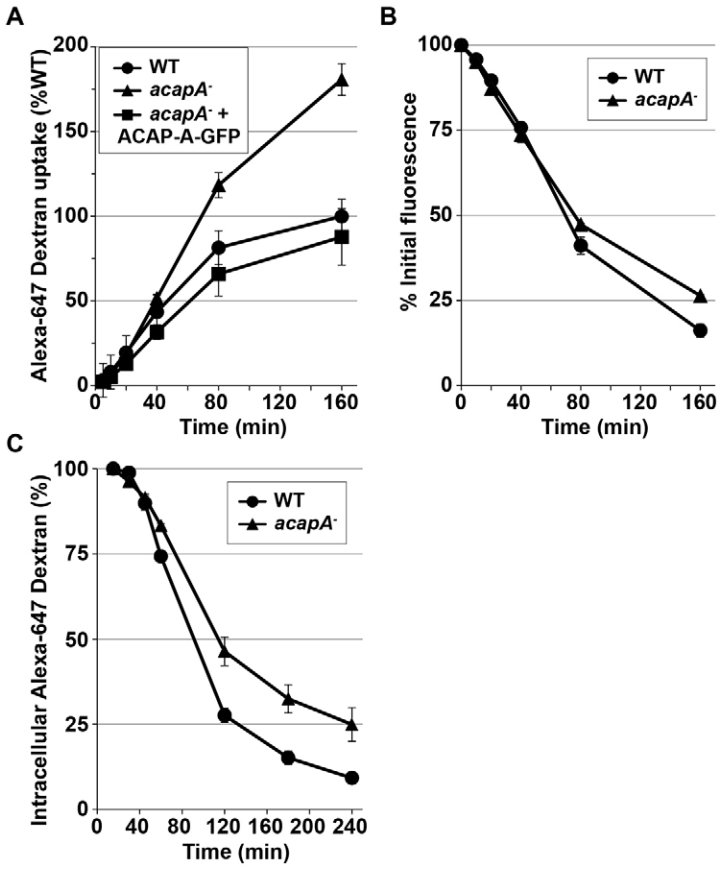

Fig. 1. Fluid-phase uptake, exocytosis, and transit in *acapA*$^-$ cells. (A) Fluid-phase uptake was monitored by incubating cells with Alexa-Fluor-643–dextran for the indicated periods of time. Fluorescence was measured by flow cytometry and data expressed as the percentage of maximal uptake in WT cells. (B) To analyze exocytosis, cells were incubated overnight with Alexa-Fluor-647-dextran to fully load all endocytic compartments, then washed and incubated with dextran-free medium. At the indicated time points, the fluorescence remaining in cells was measured by flow cytometry and expressed as the percentage of the initial fluorescence. (C) The intracellular transit time of fluid-phase markers was determined by incubation of cells with Alexa-Fluor-647-dextran for a 10-min pulse, and intracellular fluorescence was recorded after different chase periods. The percentage of maximal fluorescence for each cell type was calculated. Values in A–C are mean±s.e.m. of three independent experiments.

Journal of Cell Science (2014) 127, 4702–4713 doi:10.1242/jcs.154559

with Alexa-Fluor-647–dextran, and intracellular fluorescence was recorded after different chase periods. The half-life for internalized dextran was 90 min in WT cells, and rose to 115 min in *acapA*$^{-}$ cells (Fig. 1C). We thus conclude that the apparent increase of fluid-phase uptake observed in *acapA*$^{-}$ cells is mainly due to a prolonged transit time of internalized fluid compared to WT cells, although a minor exocytosis defect might also contribute to this increase. Interestingly, disruption of the gene encoding ACAP-B (*acapB*$^{-}$ cells) did not result in any significant defects in endocytosis (data not shown), exocytosis and intracellular transit time of fluid-phase markers (supplementary material Fig. S1A,B). These results indicate that even if ACAP-A and ACAP-B are both Arf GAPs for ArfA (Chen et al., 2010), ACAP-A has distinct functions in the endocytic pathway.

One essential step in the *D. discoideum* endocytic pathway is the neutralization of acidic lysosomes as they mature into post-lysosomes (Maniak, 2003). To determine whether the kinetics of this event was affected in the absence of ACAP-A, we first monitored lysosome neutralization by live-cell confocal microscopy. Cells were pulsed with a mixture of Oregon-Green-labeled dextran (a pH-sensitive probe) and TRITC-labeled dextran (a pH-insensitive probe) for 15 min, and chased with dextran-free culture medium for different periods of time. In this experimental setup, endosomes with neutral pH are yellow, but acidic endosomes appear red due to weak fluorescence of Oregon Green at low pH. After the pulse period, all endosomes were acidic in *acapA*$^{-}$ and WT cells. However, neutralization was delayed in *acapA*$^{-}$ cells; only 6.8% of endosomes were neutral after 35 min compared to 24.5% in WT cells (Fig. 2A, arrowheads). After 55 min, neutralization was similar in both cell types.

To analyze endosomal pH variations more precisely, we next used a previously described assay (Marchetti et al., 2009). Cells were pulsed with dextran coupled to pH-sensitive and pH-insensitive probes (Oregon Green and Alexa Fluor 647 respectively) for 10 min and chased with dextran-free culture medium. Fluorescence was analyzed here by flow cytometry, and the ratio of Oregon Green and Alexa Fluor 647 fluorescence intensities, reflecting pH variations, were calculated and compared to a pH calibration curve (Fig. 2B). In both *acapA*$^{-}$ and WT cells, early endosome acidification, during the first 20 min, occurred at a comparable rate. This first step was followed by a neutralization phase that started with a slight delay in *acapA*$^{-}$ cells compared to WT cells (starting at 25 min and 20 min, respectively). The kinetics of neutralization was also delayed in *acapA*$^{-}$ cells. Indeed, neutralization was achieved at 45 min and 35 min in *acapA*$^{-}$ and WT cells, respectively. It is noteworthy that *acapB*$^{-}$ cells did not show endosome acidification and neutralization defects (supplementary material Fig. S1C). Taken together, these results suggest that lysosomal pH neutralization is slightly and specifically affected in the absence of ACAP-A.

Phagocytosis and particle digestion defects in *acapA*$^{-}$ cells

To investigate whether ACAP-A plays a role in phagocytosis, *acapA*$^{-}$ cells were incubated with fluorescent beads and the intracellular fluorescence was measured by flow cytometry. After 20 min of incubation, *acapA*$^{-}$ and WT showed similar phagocytic rates (Fig. 3A). Furthermore, bead uptake constantly increased over time in *acapA*$^{-}$ cells (to 162.4% of the amount of phagocytosis in WT cells after 80 min) whereas a plateau was rapidly reached in WT cells after 1 h (Fig. 3A). Despite enhanced phagocytic capacities, when *acapA*$^{-}$ and WT cells were grown on

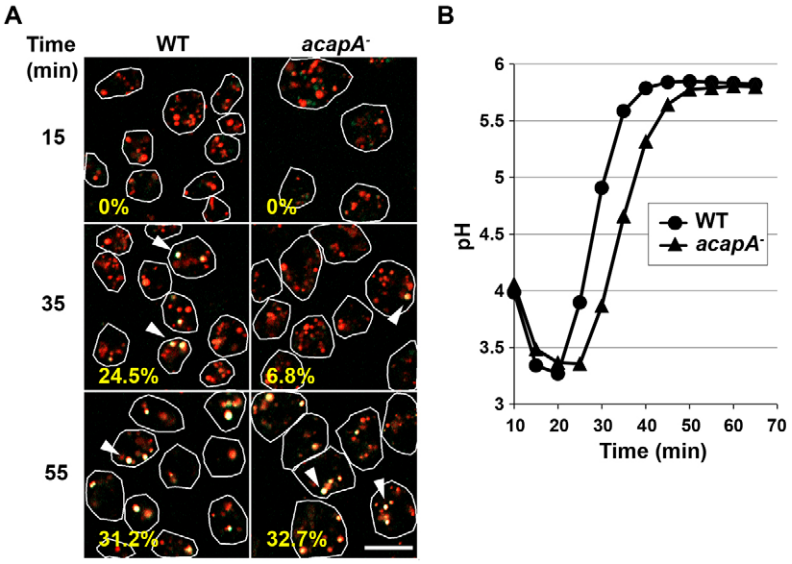

Fig. 2. Endosomal pH variations in *acapA*$^{-}$ cells. (A) To monitor pH neutralization of lysosomes, cells were incubated simultaneously with dextran coupled to Oregon Green and TRITC-conjugated dextran (which have pH-sensitive and pH-insensitive fluorescence, respectively) for 15 min. Cells were washed twice, incubated in fresh medium for the indicated times, and observed by confocal microscopy. Fifty cells were analyzed for each time point. Only one representative field is shown here. White lines indicate cell edges, and arrowheads mark examples of neutral endosomes. Numbers of endosomes were determined using the ImageJ analysis software after binary conversion of images keeping identical threshold values. The percentage of neutralized endosomes (yellow) are indicated for each time points. Scale bars: 10 μm. (B) To monitor endosomal pH variations, cells were simultaneously pulsed with dextran coupled to Oregon Green and with Alexa Fluor 647 (which have pH-sensitive and pH-insensitive fluorescence, respectively) for 10 min and chased in dextran-free culture medium for different periods of time. Fluorescence was analyzed by flow cytometry, and pH values were determined by comparison of the fluorescence ratio with a pH calibration curve. Data are from a representative experiment repeated three times with similar results.

Journal of Cell Science (2014) 127, 4702–4713 doi:10.1242/jcs.154559

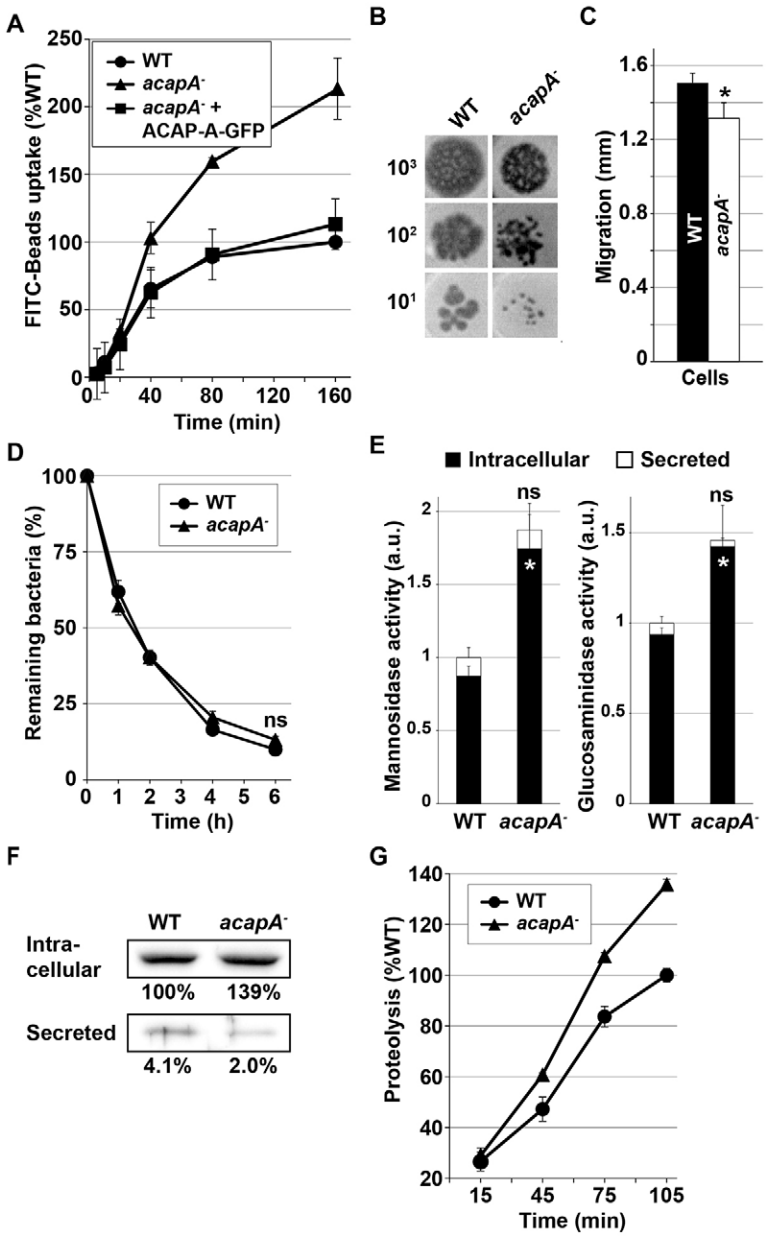

Fig. 3. Characterization of phagocytic and degradative functions in *acapA*$^{-}$ cells. (A) To determine phagocytic rates, the indicated cells were incubated with fluorescent 1-μm beads and intracellular fluorescence was analyzed for the indicated periods of time. Fluorescence was measured by flow cytometry and data expressed as the percentage of maximal uptake in WT cells. (B) The indicated number of cells were seeded on *K. pneumoniae* lawns and grown for 5 days. Phagocytic plaques (dark areas) were smaller in *acapA*$^{-}$ cells than in WT cells. (C) Chemotaxis was assayed by measuring the displacement of cells deposited on a phosphate agar plate 4 mm away from a trough filled with folate after 4 h of incubation. (D) The ability of WT and *acapA*$^{-}$ cells to kill *K. pneumoniae* was measured. Both cell lines showed similar bacteria killing efficiency. (E) The intracellular activity of lysosomal α-mannosidase and N-acetyl glucosaminidase was assessed in cellular pellets (intracellular) and in the cell culture medium (secreted) for WT and *acapA*$^{-}$ cells after 3 days of culture. Intracellular enzymatic activities were increased in *acapA*$^{-}$ cells compared to WT cells. a.u., arbitrary units. (F) After 3 days of culture, cathepsin D (44 kDa) was detected by western blot in cell pellets (intracellular) and in culture medium (secreted). Signals were quantified using the Image lab analysis software. In *acapA*$^{-}$ cells, cathepsin D accumulated intracellularly and was less efficiently secreted compared to that of WT cells. The percentage of intracellular accumulation compared to WT cells and percentage of secretion are indicated. The experiment was repeated twice with comparable results. (G) Proteolytic activity was measured by feeding cells DQ-BSA-labeled beads and measuring unquenching of the fluorophore after the indicated time of incubation. Unless indicated, all values presented here are mean±s.e.m. of at least two independent experiments. *$P<0.05$ compared with WT (Student's *t*-test); ns, not significant.

Klebsiella pneumoniae, a commonly used strain permissive for *D. discoideum* growth, phagocytic plaques were observed in both cell types; however, the diameter of phagocytic plaques was smaller in *acapA*$^{-}$ cells (Fig. 3B). This defect was not due to reduced phagocytic capacities because WT and *acapA*$^{-}$ cells showed comparable uptake of live *K. pneumonia* (supplementary material Fig. S2). Furthermore, small phagocytic plaques were also detected in *acapA*$^{-}$ cells fed upon several other bacteria strains (supplementary material Fig. S3), in agreement with a general growth defect on bacteria rather that a strain-dependent defect. In contrast, growth of *acapB*$^{-}$ cells on *K. pneumoniae* was comparable to that of WT cells (supplementary material Fig. S1D). Next we tested whether *acapA*$^{-}$ cells could properly sense bacteria. Given that folate is secreted by bacteria and acts as a chemoattractant for *D. discoideum* (Burkholder and McVeigh, 1942; Pan et al., 1972), we analyzed cell migration on non-nutrient agar in response to folate (Fig. 3C). In the absence of ACAP-A, cells were still able to sense folate; however, migration after 4 h was reduced by 12.6% compared to WT cells. Therefore, this slight chemotaxis defect might partially account for the growth defect. Alternatively, killing of internalized bacteria might be less effective in *acapA*$^{-}$ cells and/or phagosomal proteolysis of ingested bacteria might be partially defective in these cells. As shown in Fig. 3D, WT and *acapA*$^{-}$ cells were able to kill *K. pneumoniae* with similar efficiency. We also tested the enzymatic activities of some lysosomal enzymes involved in particle digestion. After 3 days of culture, we noticed increased intracellular enzymatic activities in *acapA*$^{-}$ cells compared to WT cells, whereas very low glycosidase activities were detected in the extracellular medium in all tested cells (Fig. 3E). Note that these enhanced enzymatic functions might reflect intracellular accumulation of lysosomal enzymes because the amount of cathepsin D (a lysosomal protease) substantially rose in *acapA*$^{-}$ cells, whereas extracellular secretion of cathepsin D was slightly reduced in these cells (Fig. 3F). Interestingly, only the mature form of cathepsin D was detected in WT and *acapA*$^{-}$ cells (data

Journal of Cell Science (2014) 127, 4702–4713 doi:10.1242/jcs.154559

not shown), suggesting that there was normal maturation of lysosomal enzymes in the absence of ACAP-A. Next, we measured the proteolytic activity of phagosomes in living cells using beads coupled to Alexa Fluor 594 and to BSA labeled with DQ-Green at a self-quenching concentration, which become dequenched upon proteolysis of BSA (Gopaldass et al., 2012; Le Coadic et al., 2013). We observed that protease activity was substantially increased in *acapA*$^{-}$ cells (Fig. 3G). This observation strongly suggests that active lysosomal enzymes are correctly targeted to phagosomes in *acapA*$^{-}$ cells, and their accumulation in this compartment might enhance phagosomal proteolysis capacities. Taken together, these results indicate that the slow growth rate of *acapA*$^{-}$ cells fed upon *K. pneumoniae* is not due to defects in ingestion, killing or digestion of bacteria but instead might be caused by genuine bacteria recognition problems.

Lysosome maturation is altered in *acapA*$^{-}$ cells

The above results suggested that the organization of the endocytic pathway might be defective in the absence of ACAP-A. To evaluate this possibility, *acapA*$^{-}$ cells grown in culture medium were first observed by transmission electron microscopy and compared to WT cells. The overall morphology of the *acapA*$^{-}$ cells was similar to that of WT cells (Fig. 4A). However, quantitative analysis revealed that mutant cells harbored more vacuoles per cell than WT cells (Fig. 4B). *D. discoideum* cells are characterized by the presence of acidic lysosomes that mature into neutral post-lysosomes, which can then fuse with the plasma membrane. Transmission electron microscopy observations do not allow us to distinguish between these various types of endocytic compartments. Therefore, to further characterize the endocytic pathway of *acapA*$^{-}$ cells, WT and mutant cells were loaded for 5 h with a mixture of Oregon-Green- and TRITC-labeled dextran to distinguish neutral vesicles (Fig. 5A, yellow, arrowheads) and acidic vesicles (red). Both cell types showed numerous acidic vesicles and a few neutral post-lysosomes. However, *acapA*$^{-}$ cells displayed more post-lysosomes as compared with WT cells (2.8 and 1.4 post-lysosomes per cell for *acapA*$^{-}$ and WT cells respectively, 30 cells analyzed for each cell type). To better characterize this defect, we next analyzed the endosomal distribution of F-actin, the endocytic marker p80 and the membrane H^{+}-ATPase (Neuhaus et al., 1998; Ravanel et al., 2001). In both *acapA*$^{-}$ and WT cells, lysosomes (which are H^{+}-ATPase-positive, p80-positive and F-actin-positive) (Fig. 5B, arrows) and post-lysosomes (which are H^{+}-ATPase-negative, p80-positive and F-actin-negative) (Fig. 5B, arrowheads) were both detected. The size of lysosomes was similar in both cell types, whereas post-lysosomes were significantly smaller in *acapA*$^{-}$ cells than those in WT cells (Fig. 5C). These results indicate that endocytic compartments in *acapA*$^{-}$ cells display genuine characteristics of lysosomes and post-lysosomes as tested with three relevant markers (H^{+}-ATPase, p80 and F-actin). In addition, the endocytic marker p25 (a marker of recycling endosomes in *D. discoideum*) (Ravanel et al., 2001), vacuolin (a protein binding to the surface of late endosomes; Rauchenberger et al., 1997) and two markers of the contractile vacuole (H^{+}-ATPase and Rhesus 50) (Benghezal et al., 2001; Neuhaus et al., 2002) were correctly localized in *acapA*$^{-}$ cells (data not shown), further indicating that the composition of intracellular compartments is preserved in *acapA*$^{-}$ cells.

Remarkably, *acapA*$^{-}$ cells showed an increased number of p80-positive vacuoles compared to WT cells (Fig. 5B,D). *acapA*$^{-}$ cells displayed 1.56 times more lysosomes and 2.4 times more post-lysosomes than WT cells (Fig. 5D). Moreover, the ratio between post-lysosomes and lysosomes for *acapA*$^{-}$ and WT cells (0.57 and 0.37, respectively) indicated *acapA*$^{-}$ cells have more post-lysosomes than would be expected if a normal post-lysosome:lysosome ratio was conserved. This accumulation of post-lysosomes suggested that exocytosis of these vesicles might be defective in *acapA*$^{-}$ cells. To test this hypothesis, we counted the number of p80 patches on the surface of *acapA*$^{-}$ and WT cells. These patches transiently appear upon the fusion of post-lysosomes with the plasma membrane, and are conveniently used to determine the efficiency of vesicle fusion (Charette and Cosson, 2006; Charette and Cosson, 2007). As shown in Table 1, *acapA*$^{-}$ and WT cells displayed similar number of p80 patches. However calculation of the ratio between p80 patches and post-lysosomes numbers revealed that fusion efficacy of post-lysosomes with the cell surface was actually reduced in *acapA*$^{-}$ cells (Table 1). This result supports a possible function of ACAP-A in the exocytic process. Strikingly, this post-lysosome fusion defect in *acapA*$^{-}$ cells results only in a minor fluid-phase exocytosis deficiency. This apparent discrepancy might be explained by inherent sensibility differences in assays used here to analyze these endocytic functions.

To further test the role of ACAP-A in the maturation of lysosomes, we next followed the maturation of endocytic compartments containing internalized indigestible particles in

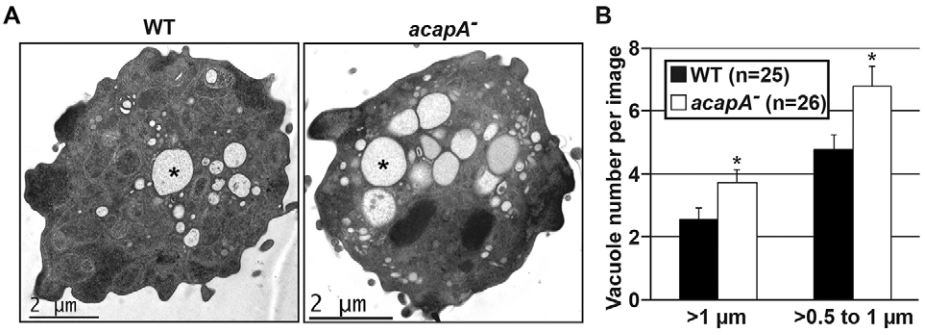

Fig. 4. Ultrastructural analysis of endocytic compartments in *acapA*$^{-}$ cells. To determine whether *acapA*$^{-}$ cells are morphologically different from WT cells, cells grown in HL5 were processed for transmission electron microscopy. (A) Representative images of WT and *acapA*$^{-}$ cells are shown. The largest vacuole in each cell type is indicated by an asterisk (*). (B) Histogram showing the number of vacuoles per image in both cell types. The values are mean±s.e.m. of vacuoles visible in images of 25 WT and 26 *acapA*$^{-}$; cells having a cell radius of at least 5 µm were analyzed. Vacuoles with a size over 1 µm and between 0.5 and 1 µm were counted (*P<0.05).

Journal of Cell Science (2014) 127, 4702–4713 doi:10.1242/jcs.154559

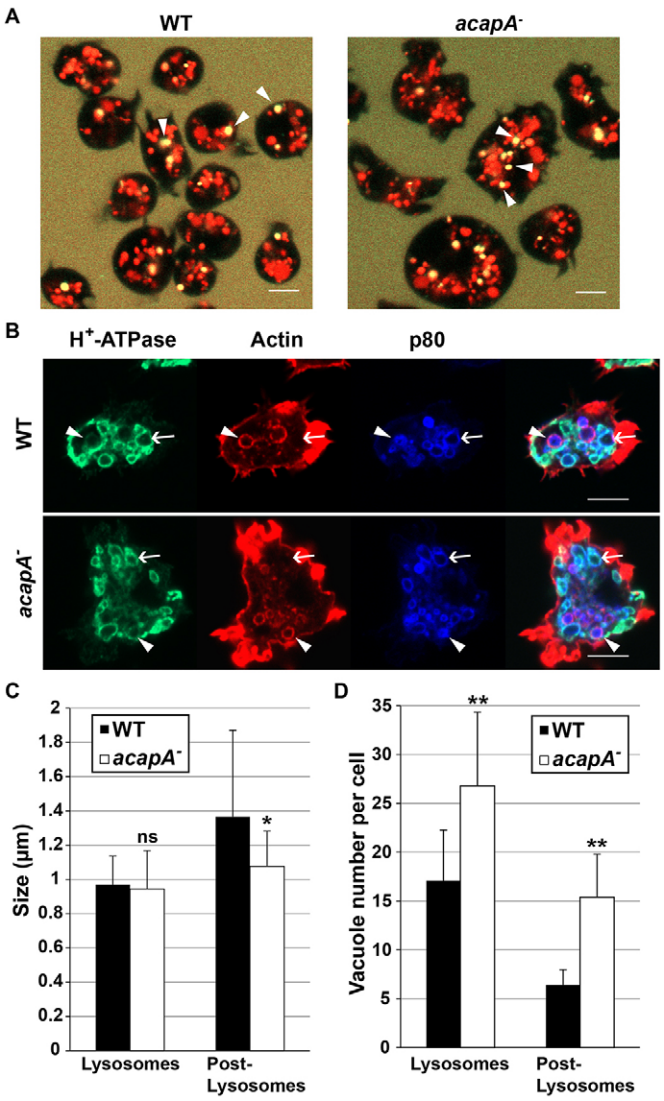

Fig. 5. Characterization of endocytic compartments in *acapA*$^{-}$ cells. (A) To identify acidic lysosomes and neutral post-lysosomes, cells were loaded for 5 h with a mixture of Oregon-Green- and TRITC-labeled dextran to distinguish neutral vesicles (yellow, arrowheads) and acidic vesicles (red), and were observed by confocal microscopy. *acapA*$^{-}$ cells displayed 2.8 post-lysosomes per cell whereas WT cells presented 1.4 post-lysosomes per cell (30 cells analyzed for each cell type). Scale bars: 10 µm. (B) Lysosomes (H^{+}-ATPase-positive, p80-positive and actin-negative; arrows) and post-lysosomes (H^{+}-ATPase-negative, p80-positive and actin-positive; arrowheads) were identified by confocal microscopy analysis. F-actin was visualized with TRITC–phalloidin. Scale bars: 5 µm. (C,D) Histogram showing the size (C) and the number (D) of lysosomes and post-lysosomes determined by the confocal microscopy analysis as described in B. Quantifications were performed using the ImageJ analysis software of microscopy confocal scans of cells from top to bottom ($n=10$ cells). *$P<0.05$; **$P<0.01$; ns, not significant.

acapA^{-} cells. Cells were pulsed with fluorescent latex beads for 15 min, and were then washed. The localization of particles in lysosomes and post-lysosomes was determined by analysis of p80 and H^{+}-ATPase markers (see representative images in Fig. 6A), and quantified after different incubation times (Fig. 6B) (Charette and Cosson, 2007; Charette and Cosson, 2008). After 30 min, most ingested particles localized to lysosomes in all tested cell lines. In WT cells, particles were efficiently transferred to post-lysosomes over the next 30 min. By contrast, in *acapA*$^{-}$ cells, transfer of particles to post-lysosomes still occurred but with slower kinetics than in WT cells, further indicative of a defect in lysosome maturation in these mutant cells. Whereas expression of ACAP-A–GFP restored the transfer of particles to post-lysosomes to normal kinetics, an ACAP-A mutant defective in the GAP activity (mutation R633Q) failed to complement the defect of *acapA*$^{-}$ cells (Fig. 6B). Therefore, the role of ACAP-A in the maturation of lysosomes might rely on the regulation of ArfA activity by this GAP. Finally, efficient transfer of particles to post-lysosomes was also observed in *acapB*$^{-}$ cells (supplementary material Fig. S1E), further highlighting the distinct functions of ACAP-A and ACAP-B.

Reduced *Legionella* intracellular growth rate in *acapA*$^{-}$ cells

Legionella pneumophila is an intracellular pathogenic bacterium that efficiently replicates in the LCVs formed in *D. discoideum* owing to bacteria-induced alteration of membrane trafficking events in this host cell (Hägele et al., 2000; Solomon et al., 2000). Because Arf is involved in the biogenesis of the LCV in macrophages (Derré and Isberg, 2004; Kagan and Roy, 2002; Kagan et al., 2004), we next tested whether the Arf GAP ACAP-A is required for intracellular growth of *L. pneumophila* in *D. discoideum*. Amoebae were infected with *L. pneumophila* (Lens strain) expressing fluorescent mCherry. After a lag period of 72 h post-infection, intracellular growth of bacteria was detected in both *acapA*$^{-}$ and WT cells as measured by mCherry fluorescence analysis (Fig. 7A). At 144 h post-infection, a 5.4-fold increase in the initial fluorescence was observed in WT cells. In contrast, bacteria growth in *acapA*$^{-}$ cells showed a marked plateau starting at 96 h, and was reduced by 34.7% compared to growth in WT cells at 144 h. Stable transfection of ACAP-A–GFP in *acapA*$^{-}$ cells restored the normal *L. pneumophila* intracellular growth rates. Note that cell infection was dependent on the bacterial type IV secretion system (T4SS) Dot/Icm because the T4SS *dotA L. pneumophila* mutant failed to replicate in all tested amoeba cells (Fig. 7A). To exclude the possibility that inhibition of *L. pneumophila* growth in *acapA*$^{-}$ cells resulted from a defect in bacteria uptake, we tested the uptake of *L. pneumophila* expressing GFP by flow cytometry. After 30 min of incubation with *L. pneumophila*, *acapA*$^{-}$ and WT cells showed similar uptake of bacteria (supplementary material Fig. S4A).

ACAP-A is not implicated in the formation of the LCV

Defects in intracellular *L. pneumophila* growth in *acapA*$^{-}$ cells suggested that the formation and the composition of LCVs might be altered in the absence of ACAP-A, thus preventing optimal replication of *L. pneumophila*. To test this hypothesis, we analyzed the presence of ER and lysosomal markers on the LCV in *acapA*$^{-}$ cells because this compartment is characterized by the presence of ER markers and the exclusion of lysosomal proteins. At 2 h post-infection, *L. pneumophila* localized in the LCVs containing the ER membrane proteins calnexin fused to GFP (Fig. 7B) and protein disulfide isomerase (PDI; data not shown) to a similar extent in both *acapA*$^{-}$ and WT cells (Fig. 7C). As previously reported (Ragaz et al., 2008; Weber et al., 2006), the endocytic marker p80 was observed on the LCV (Fig. 7D), whereas the lysosomal marker H^{+}-ATPase was only found on a minority of these vacuoles in WT cells (Fig. 7E). Such a composition was also observed in *acapA*$^{-}$ cells (Fig. 7D,E). These results strongly suggest that ACAP-A might be dispensable for the formation of the LCV.

Journal of Cell Science (2014) 127, 4702–4713 doi:10.1242/jcs.154559

Table 1. Analysis of the post-lysosome fusion rate in *acapA*$^{-}$ cells

Cell	Number of post-lysosomes per cell[a]	Number of p80 patches per cell[b]	Fusion efficacy[c]
WT	6.4±1.6	0.114±0.018	1
acapA^{-}	15.4±5.2	0.116±0.025	0.42

[a]These values are those reported Fig. 5D. [b]Number of patches per cell was determined by immunofluorescence analysis (n=500 cells) as previously described (Charette and Cosson, 2007; Charette and Cosson, 2008). Data are mean±s.e.m. of two independent experiments. [c]The fusion efficacy corresponds to the ratio between the number of p80 patches and the number of post-lysosomes per cell, normalized to that in WT cells (set at 1).

At a few hours post-infection, LCVs displaying ER markers have been described to change from a tight to a spacious morphology (Li et al., 2005b; Lu and Clarke, 2005). This morphological transition appears to be essential for efficient bacteria intracellular replication because several *D. discoideum* mutants defective in this step show reduced bacteria growth rates (Li et al., 2005b; Ragaz et al., 2008; Weber et al., 2006). Careful analysis of the LCV morphology in *acapA*$^{-}$ cells revealed no major LCV maturation defects that could account for defective *L. pneumophila* intracellular replication (data not shown).

Finally, proteomic analysis of purified LCVs has revealed that ArfA is detected 1 h post-infection and then rapidly lost (Urwyler et al., 2009), although our microscopy studies did not provide convincing evidence for the localization of ArfA–GFP on the LCV (data not shown). Given that ACAP-A is a GAP for ArfA, we next tested the localization of ACAP-A on the LCV. Analysis of WT cells expressing ACAP-A–GFP revealed that ACAP-A did not accumulate on membranes of LCVs positive for the ER marker PDI (at least 200 vacuoles were analyzed; see a representative image in supplementary material Fig. S4B) but was typically observed at the plasma membrane and the cytosol, as previously reported in non-infected WT cells (Dias et al., 2013). Although a transient recruitment of ACAP-A–GFP to the LCV cannot be formally excluded, this observation suggests that the localization of ACAP-A to the LCV is not required for the LCV biogenesis. This result is in agreement with the absence of ACAP-A in the proteome of purified LCVs previously reported (Urwyler et al., 2009).

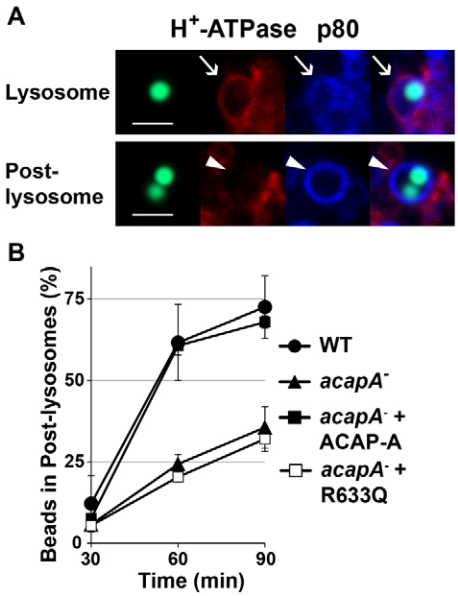

Fig. 6. Deficient transfer of latex beads from lysosomes to post-lysosomes in *acapA*$^{-}$ cells. (A) Confocal pictures of *acapA*$^{-}$ cells fed with fluorescent beads, fixed and processed to detect H^{+}-ATPase and p80 markers. Beads localized either in lysosomes (top panel; H^{+}-ATPase-positive and p80-positive compartments, arrows) or in post-lysosomes (bottom panel; H^{+}-ATPase-negative and p80-positive; arrowheads). Scale bars: 2 µm. (B) Percentage of fluorescent beads found in post-lysosomes in the indicated cell lines at different time points after a 15-min pulse with fluorescent beads. In *acapA*$^{-}$ cells, transfer of particles from lysosomes to post-lysosomes occurred but with slower kinetics than in WT cells. Expression of ACAP-A–GFP in *acapA*$^{-}$ cells restored normal transfer of particles to post-lysosomes. In contrast, an ACAP-A mutant defective in the GAP activity (mutation R633Q) failed to complement this defect. Values are mean±s.e.m. of two independent experiments (n=30 cells/time point).

ArfA regulates the intracellular growth of *L. pneumophila* and the formation of the LCV

The growth defect of *L. pneumophila* in *acapA*$^{-}$ cells prompted us to analyze the role of ArfA in intracellular growth of this bacterium because ArfA is a substrate for ACAP-A (Chen et al., 2010). ArfA-Q71L–GFP and ArfA-T31N–GFP mutants were conditionally expressed in cells 48 h before infection. These ArfA mutants mimic constitutively activated (Arf bound to GTP) and dominant-negative (Arf bound to GDP) forms of ArfA, respectively (Dias et al., 2013). In ArfA-T31N–GFP-expressing cells, *L. pneumophila* growth was reduced by 24.7% compared to growth in WT cells at 144 h post-infection (Fig. 7F). In contrast, no bacteria growth defect was observed in ArfA-Q71L–GFP-expressing cells. Moreover, the formation of the LCV was altered in ArfA-T31N–GFP-expressing cells. These cells showed a 28.8% reduction in LCVs containing the ER marker calnexin (Fig. 7G) whereas the lysosomal marker H^{+}-ATPase was still massively excluded from the LCV (data not shown).

DISCUSSION

ACAP-A and lysosome maturation

In this study, we report the role of ACAP-A, a GAP for ArfA, in the endocytic pathway of the amoeba *D. discoideum*. In the absence of ACAP-A, maturation of lysosomes into post-lysosomes is significantly perturbed, and expression of a GAP-defective ACAP-A mutant does not restore normal functions in *acapA*$^{-}$ cells. These results provide thus the first evidence that ACAP-A might play a role in lysosome maturation through an Arf-dependent activity. It is noteworthy that lysosome maturation is only partially blocked in *acapA*$^{-}$ cells. This suggests that additional factors might also regulate this process. Such a moderate lysosome maturation defect has been previously described in *lvsB*-null cells (Charette and Cosson, 2007; Charette and Cosson, 2008). LvsB is *D. discoideum* ortholog of mammalian lysosomal trafficking regulator (LYST) and regulates the fusion between lysosomes and post-lysosomes (Kypri et al., 2013). In contrast, more severe lysosome maturation defects have been reported in two other well-characterized mutants, µ3- and

Journal of Cell Science (2014) 127, 4702–4713 doi:10.1242/jcs.154559

WASH-null cells, both of which are impaired in vesicle fission events. Hence, cells lacking the μ3 subunit of the AP-3 clathrin adaptor complex show defects in protein recycling from early endosomes because of a vesicle-fission-dependent mechanism that results in major defects along the endocytic pathway (Charette and Cosson, 2006; Charette and Cosson, 2008). Moreover, in the absence of the nucleation-promoting factor WASH, the removal of H^+-ATPase from late lysosomes is impaired and neutralization of lysosomes to form post-lysosomes is fully inhibited (Carnell et al., 2011). In contrast to WASH-null cells, neutralization of lysosomes containing a pH-sensitive fluid-phase marker still occurs in *acapA*$^-$ cells but with reduced kinetics. This result strongly suggests that ACAP-A might only partially control the retrieval of H^+-ATPase from lysosomes leading to pH neutralization. The retrieval of H^+-ATPase from maturing lysosomes relies on vesicles (Clarke et al., 2010) whose biogenesis depends on actin polymerization driven by WASH (Carnell et al., 2011). Because ACAP-A has been shown to regulate the actin cytoskeleton dynamics in an ArfA-dependent manner (Dias et al., 2013), we propose that ArfA and ACAP-A could also participate in the control of actin polymerization on these recycling vesicles by regulating the activity of actin nucleation-promoting factors such as WASH. In agreement with this hypothesis, mammalian Arf1 has been recently shown to cooperate *in vitro* with the Rho GTPase Rac1 to fully activate the WAVE regulatory complex that controls actin polymerization to

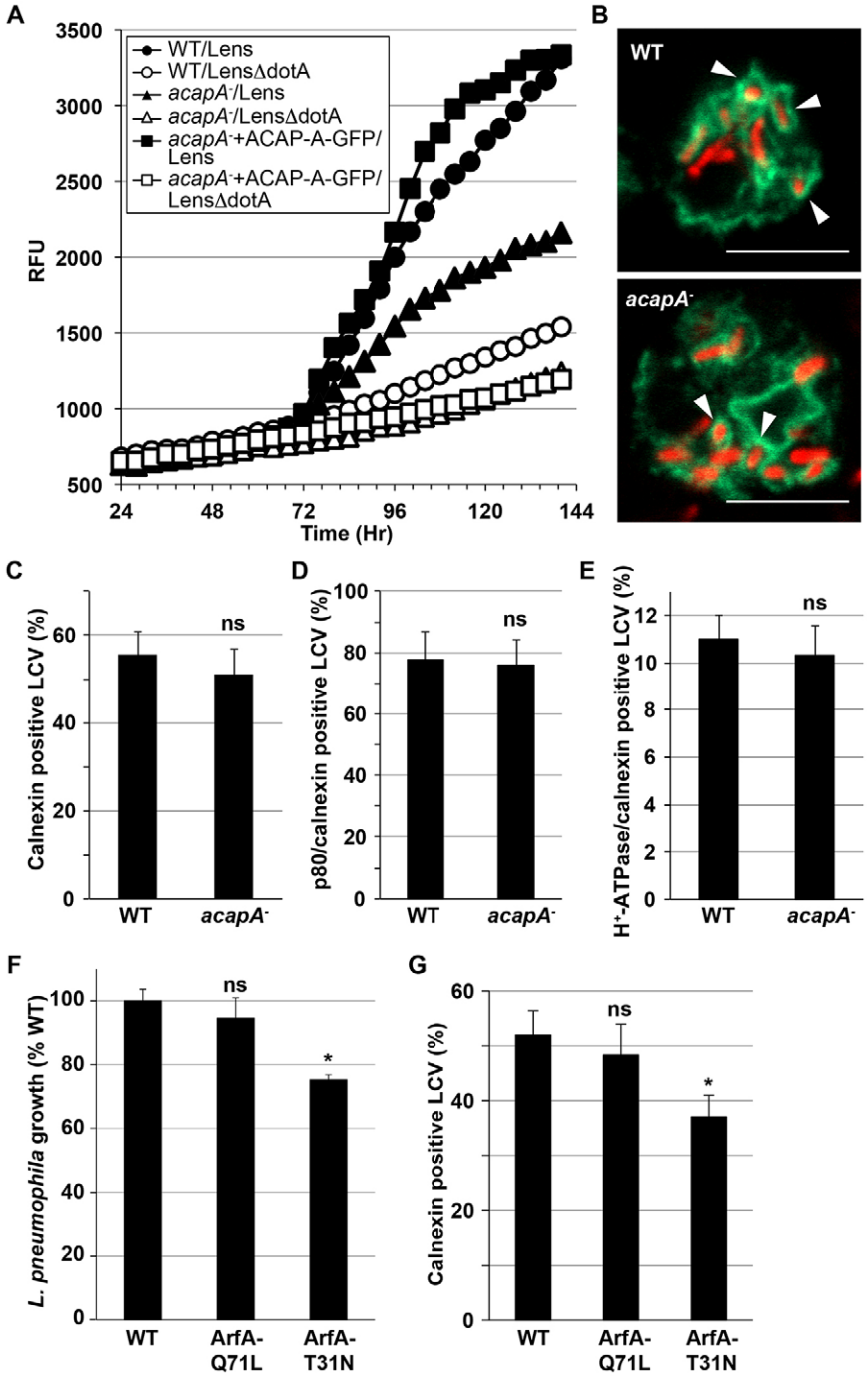

Fig. 7. Defective replication of *L. pneumophila* in *acapA*$^-$ cells. (A) Intracellular growth of *L. pneumophila* in amoebae. The indicated cells were infected at an MOI of 10 by *L. pneumophila* (Lens strain and T4SS *dotA* mutant) expressing mCherry, and replication was monitored by measuring fluorescence over time (RFU, relative fluorescence units). In *acapA*$^-$ cells, bacteria replication showed a plateau starting at 96 h, and was reduced by 34.7% compared to growth in WT cells at 144 h. (B) Characterization of the LCV in *acapA*$^-$ cells. The indicated cells expressing calnexin–GFP (an ER marker) were infected by *L. pneumophila* expressing mCherry. At 2 h post-infection, cells were fixed and analyzed by confocal microscopy. Arrowheads indicate LCVs (red) decorated with calnexin–GFP (green). Scale bars: 10 μm. (C–E) Quantification of LCVs positive for calnexin–GFP (C), p80 (D) and H^+-ATPase (E) markers in *acapA*$^-$ and WT cells at 2 h post-infection. Infected cells were fixed, and processed for immunofluorescence. Values are mean±s.e.m. of two independent experiments (n=200 LCVs); ns, not significant. In both cell types, p80 was observed on LCVs. In contrast, the endosomal H^+-ATPase was efficiently excluded from these vacuoles in *acapA*$^-$ and WT cells. (F) Intracellular growth of *L. pneumophila* in ArfA mutant cells. Wild-type (WT) cells, or cells expressing ArfA-Q71L–GFP and ArfA-T31N–GFP were infected by *L. pneumophila* expressing mCherry. Replication was monitored as in A, and expressed as the percentage of bacteria growth observed in WT cells at 144 h post-infection. In ArfA-T31N–GFP-expressing cells, bacteria replication was reduced by 24.7% compared to growth in WT cells at 144 h. *P<0.05; ns, not significant. This experiment was repeated twice with comparable results. (G) Quantification of LCVs positive for the ER marker calnexin in ArfA mutant cells. The indicated cells were infected by *L. pneumophila* expressing mCherry. At 1 h post-infection, cells were fixed, processed for immunofluorescence with an anti-calnexin antibody and analyzed by confocal microscopy. ArfA-T31N–GFP-expressing cells showed a 28.8% reduction in LCVs containing calnexin. Values are mean±s.e.m. of two independent experiments (n=200 LCVs). *P<0.05; ns, not significant.

Journal of Cell Science (2014) 127, 4702–4713 doi:10.1242/jcs.154559

membranes (Koronakis et al., 2011). More detailed studies, especially at the single-cell level using live-cell microscopy to record trafficking of fluorescently-tagged key proteins (e.g. H^+-ATPase and WASH), will be required to further determine the precise function of ACAP-A in lysosome maturation.

Additional functions for ACAP-A

In addition to lysosome maturation, our results suggest that ACAP-A might play a role in fusion of post-lysosomes with the plasma membrane. Hence, *acapA*$^-$ cells show a reduced rate of fusion of post-lysosomes with the cell surface leading to accumulation of post-lysosomes. Although ACAP-A might control some important steps in the membrane fusion process per se, we favor the hypothesis that ACAP-A might control the fusion competency of post-lysosomes or the targeting of post-lysosomes to the plasma membrane. For instance, ACAP-A might regulate tethering factors involved in vesicle docking to the plasma membrane, such as the exocyst complex (Hsu et al., 1996; TerBush et al., 1996). Consistent with this hypothesis, Arf6 has been shown to associate and regulate the exocyst during endocytic membrane recycling in mammalian cells (Prigent et al., 2003). Although the molecular mechanism of exocytosis is unknown in *D. discoideum*, a yeast two-hybrid screen with Sec15 (an exocyst subunit) has revealed highly that it interacts with ArfA (Essid et al., 2012), in accordance with the proposed regulatory function of ACAP-A in vesicle docking during exocytosis.

ACAP-A and pathogen host cell defense

Here, we show that intracellular replication of *L. pneumophila* is partially inhibited in *acapA*$^-$ cells, but that the morphology and the composition of the LCV still appear to be intact. This normal biogenesis of the LCV in *acapA*$^-$ cells indicates that ACAP-A is dispensable for the formation of the replicative niche. In macrophages, Arf1 plays essential functions of in the formation of the LCV (Derré and Isberg, 2004; Kagan and Roy, 2002; Kagan et al., 2004). Here, we found that expression of a dominant-negative variant of ArfA in *D. discoideum* affects both the growth of *L. pneumophila* and the formation of the LCV. This LCV biogenesis defect is similar to that described in macrophages overexpressing the Arf1 dominant-negative variant Arf1-T31N–GFP (Kagan and Roy, 2002). We thus provide the first evidence that ArfA might play a role similar to Arf1 in cells infected with *D. discoideum*. Although ArfA mutants might not fully simulate the actual fine-tuning of ArfA activity, our results suggest that ArfA might be in an activated state (GTP-bound) to support the LCV biogenesis. Accordingly, we observe that the lack of ACAP-A in *acapA*$^-$ cells, inferred to induce excess activated ArfA, does not impede the formation of the LCV. So, why is the replication of *L. pneumophila* inhibited in *acapA*$^-$ cells in the absence of defects in LCV biogenesis? Although proteomic analysis of the LCV composition in *acapA*$^-$ cells would probably give some hints for answering this question, the ACAP-A functions in the endocytic pathway revealed here might also readily provide interesting clues on the role of ArfA and ACAP-A in *L. pneumophila* intracellular replication. Indeed, our results point to a role of ACAP-A in the control of actin dynamics, and this function might be essential for optimal intracellular growth of *L. pneumophila*. In agreement with this hypothesis, mounting evidence reveals that the actin cytoskeleton dynamics plays a fundamental role in *L. pneumophila* virulence (Franco and Shuman, 2012). Besides classical functions in the uptake mechanism by host cells and its presence on the LCV at later times post-infection, actin has recently been shown to be the target of the *L. pneumophila* effector VipA. This bacterial effector binds and nucleates actin polymerization *in vitro* and it associates with actin filaments and early endosomes during macrophage infection (Franco et al., 2012). The control of actin dynamics by VipA is thought to interfere with host cell organelle trafficking pathways, preventing deleterious connections of the LCV with the endocytic machinery. This report on VipA identifies actin as a key factor in *L. pneumophila* virulence, hence ACAP-A might be an important regulatory element in actin-dependent steps. Alternatively (or in addition) to the modulation of actin dynamics, the role of ACAP-A in *L. pneumophila* virulence could rely on other well-known Arf activities. Among those, Arf proteins have been described to regulate vesicular traffic and phospholipid metabolism (D'Souza-Schorey and Chavrier, 2006; Donaldson and Jackson, 2011; Gillingham and Munro, 2007). These functions are essential for *L. pneumophila* infection. For instance, several translocated effectors have been described to bind phosphoinositides on the LCV and promote a modification in lipid membrane composition required for the LCV biogenesis (Haneburger and Hilbi, 2013).

Finally, the *L. pneumophila* infection mechanisms in *D. discoideum* and human macrophages are highly comparable (Hägele et al., 2000; Solomon et al., 2000). Therefore, mammalian Arf GAPs homologous to ACAP-A might play similar roles in *L. pneumophila* infection of macrophages. There are three different mammalian ACAPs with high similarity to ACAP-A (Gillingham and Munro, 2007; Chen et al., 2010). Given that ACAP1 and ACAP2 have preferential GAP activities towards Arf6 *in vivo* (Jackson et al., 2000), an involvement in *L. pneumophila* infection seems unlikely. ACAP3 has not been characterized yet. In addition to ACAPs, ACAP-A also shares a domain organization comparable to mammalian ASAPs, which also have with BAR, PH, Arf GAP and ankyrin repeat domains (Gillingham and Munro, 2007; Chen et al., 2010). Interestingly, ASAP1 has been shown to function as a GAP for Arf1 *in vivo* (Furman et al., 2002), a requisite for a hypothetic role in *L. pneumophila* infection. Further studies will be needed to evaluate the functions of ACAPs and ASAPs during *L. pneumophila* infection of macrophages.

MATERIALS AND METHODS

Amoebae and bacteria strains

D. discoideum strain DH1-10 (Cornillon et al., 2000), and mutants *acapA*$^-$ and *acapB*$^-$ (Dias et al., 2013) were grown at 22℃ in HL5 medium. Plasmids encoding calnexin–GFP (Müller-Taubenberger et al., 2001), ACAP-A–GFP and the ACAP-A–GFP mutant R633Q (Dias et al., 2013) were transfected in cells by electroporation as reported previously (Alibaud et al., 2003). ArfA(Q71L) and ArfA(T31N) mutants cloned in the inducible expression vector pDM370 were as previously described (Dias et al., 2013). Expression was induced by adding 10 mg/ml doxycycline 2 or 3 days before analysis. *L. pneumophila* strains (virulent *L. pneumophila* serogroup 1, strain Lens, and avirulent *dotA* mutant Lens *lpl2613*::Km) were grown at 30℃ on buffered charcoal yeast extract (BCYE) agar or in BYE liquid medium. The laboratory strain of *K. pneumonia* (Benghezal et al., 2006) was grown overnight at 37℃ in LB medium.

Internalization

Internalization of fluid phase (Alexa-Fluor-647–dextran; Molecular Probes, Eugene, OR) or phagocytic particles (FITC-conjugated fluorescent 1-µm diameter latex beads; Polysciences, Warrington, PA) was carried out as previously described (Lima et al., 2012) and

analyzed by flow cytometry (FACS Calibur, Becton Dickinson, San Jose, CA).

Uptake of *L. pneumophila* strains by *D. discoideum* was analyzed by flow cytometry using GFP-labeled bacteria. *L. pneumophila* cells harboring a plasmid expressing GFP were grown on BYE liquid medium containing 2 mM IPTG and chloramphenicol for 4 days at 30℃. Amoeba were seeded in 24-well microplates (5×10^5 cells per well) and then infected with 5×10^7 fluorescent *L. pneumophila* [multiplicity of infection (MOI)=100]. Infection was synchronized by centrifuging bacteria at 880 ***g*** for 10 min and plates were incubated 20 min at 25℃. Extracellular bacteria were removed by washing three times with SorC (2 mM Na_2HPO_4, 15 mM KH_2PO_4, 50 µM $CaCl_2$, pH 6.0). Infected cells were detached in HL5 containing 0.2% azide by vigorously pipetting. Cells were then centrifuged at 3000 ***g*** for 1 min and resuspended in 0.5 ml of HL5 medium containing 0.5% paraformaldehyde.

Transmission electron microscopy

DH1-10 and *acapA*$^-$ cells grown in HL5 were fixed for 3 h in 0.1 M sodium cacodylate buffer (pH 7.3) containing 2% glutaraldehyde and 0.3% osmium tetroxide and then processed for transmission electron microscopy as previously described (Paquet et al., 2013). Samples were examined using a transmission electron microscope (JEOL 1230) at 80 kV.

Antibodies and immunofluorescence microscopy

Antibodies against protein disulfide isomerase (221-64-1, mouse monoclonal), p80 (H161 mouse monoclonal), cathepsin D and vacuolar H^+-ATPase (221-35-2, mouse monoclonal) were as described previously (Journet et al., 1999; Monnat et al., 1997; Neuhaus et al., 1998; Ravanel et al., 2001). Actin was labeled using tetramethylrhodamine B isothiocyanate (TRITC)-labeled phalloidin (Sigma-Aldrich, St Quentin Fallavier, France). For immunofluorescence analysis, cells were applied on glass coverslips for 3 h, then fixed with 4% paraformaldehyde for 30 min, washed and permeabilized with 0.1% Triton X-100 for 10 min. Cells were incubated with the indicated antibodies for 1 h, and then stained with appropriate fluorescent (Alexa Fluor 488, 568 or 633) secondary antibodies (Molecular Probes, Invitrogen, Eugene, OR) for 30 min. When required, anti-p80 monoclonal antibody directly coupled to Alexa Fluor 633 was used. Cells were observed by laser scanning confocal microscopy (Zeiss LSM 510). The quantification of the number and diameter of lysosomes and post-lysosomes, and kinetics of lysosome maturation (pH neutralization) were carried out as already described (Charette and Cosson, 2007). The visualization of neutral post-lysosomes was performed using dextran coupled to Oregon Green and TRITC-conjugated dextran (pH-sensitive and pH-insensitive dextran, respectively) as previously described (Jenne et al., 1998; Rivero and Maniak, 2006). Briefly, cells were seeded onto glass-bottomed dishes and incubated in LoFlo medium for 1 h. Cells were then pulsed with LoFlo medium containing 4 mg/ml Oregon-Green–dextran and 40 mg/ml TRITC–dextran for 15 min. Cells were washed twice, incubated in fresh LoFlo medium for the indicated times, and observed by confocal microscopy. For immunofluorescence analysis of cells infected with *L. pneumophila, D. discoideum* cells were seeded on coverslips, incubated overnight, and then infected with fluorescent *L. pneumophila* (MOI=100). After centrifugation (880 ***g*** for 10 min) to initiate cell–bacterium contact, cells were incubated at 25℃ for the indicated times. Coverslips were then processed for immunofluorescence as described above.

Bacteria killing, chemotaxis, glycosidase activities and phagosomal proteolysis

The ability of *D. discoideum* strains to kill internalized *Klebsiella* bacteria was tested as described previously (Benghezal et al., 2006). *D. discoideum* growth on bacteria lawn was tested as reported (Froquet et al., 2009). Chemotaxis was assayed using a semi-quantitative assay (Wallace and Frazier, 1979). Briefly, cells were first starved in phosphate buffer for 6 h, and then 1 µl of 2.5×10^8 cells/ml was deposited on a phosphate agar (1.6%) plate, 4 mm away from a trough filled with 250 µM folate. After 4 h at 22℃, migration distances were calculated by measuring displacement of cell front. Glycosidase activities (N-acetyl β-glucosaminidase and α-mannosidase) and cathepsin D content in cell pellet and culture medium after 3 days of culture were assessed as previously described (Froquet et al., 2008; Le Coadic et al., 2013). For enzymatic activities and western immunoblot analysis, equal amounts of protein were analyzed. Phagosomal proteolysis of DQ-BSA-labeled beads was determined as reported previously (Gopaldass et al., 2012; Le Coadic et al., 2013). After bead uptake, the cell suspension was analyzed by flow cytometry to determine the intensity of the DQ-green fluorescent marker in cells containing phagocytosed beads (Le Coadic et al., 2013).

Intracellular replication

Monitoring of *L. pneumophila* intracellular growth in *D. discoideum* was adapted from an assay described previously (Hervet et al., 2011). *L. pneumophila* bacteria harboring a plasmid expressing mCherry were grown on BYE liquid medium containing 2 mM IPTG and chloramphenicol for 4 days at 30℃. *D. discoideum* cells were seeded in 96-well microplates (10^5 cells/well) and then infected with 10^6 fluorescent *L. pneumophila* (MOI=10). Infection was synchronized by centrifuging plates at 880 ***g*** for 10 min. Plates were further incubated for 1 h at 25℃ and then washed three times. Intracellular growth was automatically monitored by measuring the fluorescence of mCherry at an excitation of 580 nm and an emission of 620 nm in an Infinite 200 Pro plate reader every hour for 144 h (TECAN, Männedorf, Switzerland).

Acknowledgements

We thank Virginie Molle (UMR5235, Montpellier, France) for hosting this project in her laboratory. We also wish to thank Richard Janvier (Electron microscopy platform of Institut de Biologie Intégrative et des Systèmes) for his technical assistance.

Competing interests

The authors declare no competing interests.

Author contributions

N.B. performed and analyzed *L. pneumophila* experiments. P.C. performed and analyzed phagosomal proteolytic activity experiments. S.J.C. and V.E.P. performed and analyzed electron microscopy studies. S.J.C wrote the paper. P.D. analyzed *L. pneumophila* experiments and wrote the paper. F.L. conceived of the study, performed the majority of the experiments and wrote the paper.

Funding

This work was funded by the Centre National de la Recherche Scientifique (CNRS); the Institut National de la Recherche Médicale (INSERM); the Université Lyon 1; and by grants (to F.L.) from the Association pour la Recherche contre le Cancer (ARC). The P.C. laboratory was supported by the Swiss National Foundation for Scientific Research [grant number 31003A-153326]; and the Fondation Egon Naef pour la Recherche in Vitro. The S.J.C. laboratory was supported by a grant from the Chaire de pneumologie de la fondation J.-D. Bégin de l'Université Laval et le Fonds Alphonse L'Espérance de la fondation de l'IUCPQ. This work was performed within the framework of the LABEX ECOFECT [grant number ANR-11-LABX-0042] of Université de Lyon, within the program 'Investissements d'Avenir' [grant number ANR-11-IDEX-0007] operated by the French National Research Agency (ANR).

Supplementary material

Supplementary material available online at
http://jcs.biologists.org/lookup/suppl/doi:10.1242/jcs.154559/-/DC1

References

Alibaud, L., Cosson, P. and Benghezal, M. (2003). Dictyostelium discoideum transformation by oscillating electric field electroporation. *Biotechniques* **35**, 78-80, 82-83.

Allombert, J., Fuche, F., Michard, C. and Doublet, P. (2013). Molecular mimicry and original biochemical strategies for the biogenesis of a Legionella pneumophila replicative niche in phagocytic cells. *Microbes Infect.* **15**, 981-988.

Benghezal, M., Gotthardt, D., Cornillon, S. and Cosson, P. (2001). Localization of the Rh50-like protein to the contractile vacuole in Dictyostelium. *Immunogenetics* **52**, 284-288.

Benghezal, M., Fauvarque, M. O., Tournebize, R., Froquet, R., Marchetti, A., Bergeret, E., Lardy, B., Klein, G., Sansonetti, P., Charette, S. J. et al. (2006). Specific host genes required for the killing of Klebsiella bacteria by phagocytes. *Cell. Microbiol.* **8**, 139-148.

Burkholder, P. R. and McVeigh, I. (1942). Synthesis of Vitamins by Intestinal Bacteria. *Proc. Natl. Acad. Sci. USA* **28**, 285-289.

Carnell, M., Zech, T., Calaminus, S. D., Ura, S., Hagedorn, M., Johnston, S. A., May, R. C., Soldati, T., Machesky, L. M. and Insall, R. H. (2011). Actin polymerization driven by WASH causes V-ATPase retrieval and vesicle neutralization before exocytosis. *J. Cell Biol.* **193**, 831-839.

Charette, S. J. and Cosson, P. (2006). Exocytosis of late endosomes does not directly contribute membrane to the formation of phagocytic cups or pseudopods in Dictyostelium. *FEBS Lett.* **580**, 4923-4928.

Charette, S. J. and Cosson, P. (2007). A LYST/beige homolog is involved in biogenesis of Dictyostelium secretory lysosomes. *J. Cell Sci.* **120**, 2338-2343.

Charette, S. J. and Cosson, P. (2008). Altered composition and secretion of lysosome-derived compartments in Dictyostelium AP-3 mutant cells. *Traffic* **9**, 588-596.

Chen, P. W., Randazzo, P. A. and Parent, C. A. (2010). ACAP-A/B are ArfGAP homologs in dictyostelium involved in sporulation but not in chemotaxis. *PLoS ONE* **5**, e8624.

Clarke, M., Maddera, L., Engel, U. and Gerisch, G. (2010). Retrieval of the vacuolar H-ATPase from phagosomes revealed by live cell imaging. *PLoS ONE* **5**, e8585.

Cornillon, S., Pech, E., Benghezal, M., Ravanel, K., Gaynor, E., Letourneur, F., Brückert, F. and Cosson, P. (2000). Phg1p is a nine-transmembrane protein superfamily member involved in dictyostelium adhesion and phagocytosis. *J. Biol. Chem.* **275**, 34287-34292.

D'Souza-Schorey, C. and Chavrier, P. (2006). ARF proteins: roles in membrane traffic and beyond. *Nat. Rev. Mol. Cell Biol.* **7**, 347-358.

Derré, I. and Isberg, R. R. (2004). Legionella pneumophila replication vacuole formation involves rapid recruitment of proteins of the early secretory system. *Infect. Immun.* **72**, 3048-3053.

Dias, M., Blanc, C., Thazar-Poulot, N., Ben Larbi, S., Cosson, P. and Letourneur, F. (2013). Dictyostelium ACAP-A is an ArfGAP involved in cytokinesis, cell migration and actin cytoskeleton dynamics. *J. Cell Sci.* **126**, 756-766.

Donaldson, J. G. and Jackson, C. L. (2011). ARF family G proteins and their regulators: roles in membrane transport, development and disease. *Nat. Rev. Mol. Cell Biol.* **12**, 362-375.

Essid, M., Gopaldass, N., Yoshida, K., Merrifield, C. and Soldati, T. (2012). Rab8a regulates the exocyst-mediated kiss-and-run discharge of the Dictyostelium contractile vacuole. *Mol. Biol. Cell* **23**, 1267-1282.

Franco, I. S. and Shuman, H. A. (2012). A pathogen's journey in the host cell: Bridges between actin and traffic. *BioArchitecture* **2**, 38-42.

Franco, I. S., Shohdy, N. and Shuman, H. A. (2012). The Legionella pneumophila effector VipA is an actin nucleator that alters host cell organelle trafficking. *PLoS Pathog.* **8**, e1002546.

Froquet, R., Cherix, N., Birke, R., Benghezal, M., Cameroni, E., Letourneur, F., Mösch, H. U., De Virgilio, C. and Cosson, P. (2008). Control of cellular physiology by TM9 proteins in yeast and Dictyostelium. *J. Biol. Chem.* **283**, 6764-6772.

Froquet, R., Lelong, E., Marchetti, A. and Cosson, P. (2009). Dictyostelium discoideum: a model host to measure bacterial virulence. *Nat. Protoc.* **4**, 25-30.

Furman, C., Short, S. M., Subramanian, R. R., Zetter, B. R. and Roberts, T. M. (2002). DEF-1/ASAP1 is a GTPase-activating protein (GAP) for ARF1 that enhances cell motility through a GAP-dependent mechanism. *J. Biol. Chem.* **277**, 7962-7969.

Gillingham, A. K. and Munro, S. (2007). The small G proteins of the Arf family and their regulators. *Annu. Rev. Cell Dev. Biol.* **23**, 579-611.

Gopaldass, N., Patel, D., Kratzke, R., Dieckmann, R., Hausherr, S., Hagedorn, M., Monroy, R., Krüger, J., Neuhaus, E. M., Hoffmann, E. et al. (2012). Dynamin A, Myosin IB and Abp1 couple phagosome maturation to F-actin binding. *Traffic* **13**, 120-130.

Hägele, S., Köhler, R., Merkert, H., Schleicher, M., Hacker, J. and Steinert, M. (2000). Dictyostelium discoideum: a new host model system for intracellular pathogens of the genus Legionella. *Cell. Microbiol.* **2**, 165-171.

Haneburger, I. and Hilbi, H. (2013). Phosphoinositide lipids and the Legionella pathogen vacuole. *Curr. Top. Microbiol. Immunol.* **376**, 155-173.

Hervet, E., Charpentier, X., Vianney, A., Lazzaroni, J. C., Gilbert, C., Atlan, D. and Doublet, P. (2011). Protein kinase LegK2 is a type IV secretion system effector involved in endoplasmic reticulum recruitment and intracellular replication of Legionella pneumophila. *Infect. Immun.* **79**, 1936-1950.

Hsu, S. C., Ting, A. E., Hazuka, C. D., Davanger, S., Kenny, J. W., Kee, Y. and Scheller, R. H. (1996). The mammalian brain rsec6/8 complex. *Neuron* **17**, 1209-1219.

Inoue, H. and Randazzo, P. A. (2007). Arf GAPs and their interacting proteins. *Traffic* **8**, 1465-1475.

Jackson, T. R., Brown, F. D., Nie, Z., Miura, K., Foroni, L., Sun, J., Hsu, V. W., Donaldson, J. G. and Randazzo, P. A. (2000). ACAPs are arf6 GTPase-activating proteins that function in the cell periphery. *J. Cell Biol.* **151**, 627-638.

Jenne, N., Rauchenberger, R., Hacker, U., Kast, T. and Maniak, M. (1998). Targeted gene disruption reveals a role for vacuolin B in the late endocytic pathway and exocytosis. *J. Cell Sci.* **111**, 61-70.

Journet, A., Chapel, A., Jehan, S., Adessi, C., Freeze, H., Klein, G. and Garin, J. (1999). Characterization of Dictyostelium discoideum cathepsin D. *J. Cell Sci.* **112**, 3833-3843.

Kagan, J. C. and Roy, C. R. (2002). Legionella phagosomes intercept vesicular traffic from endoplasmic reticulum exit sites. *Nat. Cell Biol.* **4**, 945-954.

Kagan, J. C., Stein, M. P., Pypaert, M. and Roy, C. R. (2004). Legionella subvert the functions of Rab1 and Sec22b to create a replicative organelle. *J. Exp. Med.* **199**, 1201-1211.

King, J. S., Gueho, A., Hagedorn, M., Gopaldass, N., Leuba, F., Soldati, T. and Insall, R. H. (2013). WASH is required for lysosomal recycling and efficient autophagic and phagocytic digestion. *Mol. Biol. Cell* **24**, 2714-2726.

Kobayashi, H. and Fukuda, M. (2012). Rab35 regulates Arf6 activity through centaurin-β2 (ACAP2) during neurite outgrowth. *J. Cell Sci.* **125**, 2235-2243.

Kobayashi, H. and Fukuda, M. (2013). Rab35 establishes the EHD1-association site by coordinating two distinct effectors during neurite outgrowth. *J. Cell Sci.* **126**, 2424-2435.

Koronakis, V., Hume, P. J., Humphreys, D., Liu, T., Hørning, O., Jensen, O. N. and McGhie, E. J. (2011). WAVE regulatory complex activation by cooperating GTPases Arf and Rac1. *Proc. Natl. Acad. Sci. USA* **108**, 14449-14454.

Kypri, E., Falkenstein, K. and De Lozanne, A. (2013). Antagonistic control of lysosomal fusion by Rab14 and the Lyst-related protein LvsB. *Traffic* **14**, 599-609.

Lamoth, F. and Greub, G. (2010). Amoebal pathogens as emerging causal agents of pneumonia. *FEMS Microbiol. Rev.* **34**, 260-280.

Le Coadic, M., Froquet, R., Lima, W. C., Dias, M., Marchetti, A. and Cosson, P. (2013). Phg1/TM9 proteins control intracellular killing of bacteria by determining cellular levels of the Kil1 sulfotransferase in Dictyostelium. *PLoS ONE* **8**, e53259.

Li, J., Ballif, B. A., Powelka, A. M., Dai, J., Gygi, S. P. and Hsu, V. W. (2005a). Phosphorylation of ACAP1 by Akt regulates the stimulation-dependent recycling of integrin beta1 to control cell migration. *Dev. Cell* **9**, 663-673.

Li, Z., Solomon, J. M. and Isberg, R. R. (2005b). Dictyostelium discoideum strains lacking the RtoA protein are defective for maturation of the Legionella pneumophila replication vacuole. *Cell. Microbiol.* **7**, 431-442.

Li, J., Peters, P. J., Bai, M., Dai, J., Bos, E., Kirchhausen, T., Kandror, K. V. and Hsu, V. W. (2007). An ACAP1-containing clathrin coat complex for endocytic recycling. *J. Cell Biol.* **178**, 453-464.

Lima, W. C., Leuba, F., Soldati, T. and Cosson, P. (2012). Mucolipin controls lysosome exocytosis in Dictyostelium. *J. Cell Sci.* **125**, 2315-2322.

Lu, H. and Clarke, M. (2005). Dynamic properties of Legionella-containing phagosomes in Dictyostelium amoebae. *Cell. Microbiol.* **7**, 995-1007.

Maniak, M. (2003). Fusion and fission events in the endocytic pathway of Dictyostelium. *Traffic* **4**, 1-5.

Marchetti, A., Lelong, E. and Cosson, P. (2009). A measure of endosomal pH by flow cytometry in Dictyostelium. *BMC Res. Notes* **2**, 7.

Monnat, J., Hacker, U., Geissler, H., Rauchenberger, R., Neuhaus, E. M., Maniak, M. and Soldati, T. (1997). Dictyostelium discoideum protein disulfide isomerase, an endoplasmic reticulum resident enzyme lacking a KDEL-type retrieval signal. *FEBS Lett.* **418**, 357-362.

Müller-Taubenberger, A., Lupas, A. N., Li, H., Ecke, M., Simmeth, E. and Gerisch, G. (2001). Calreticulin and calnexin in the endoplasmic reticulum are important for phagocytosis. *EMBO J.* **20**, 6772-6782.

Nagai, H., Kagan, J. C., Zhu, X., Kahn, R. A. and Roy, C. R. (2002). A bacterial guanine nucleotide exchange factor activates ARF on Legionella phagosomes. *Science* **295**, 679-682.

Neuhaus, E. M., Horstmann, H., Almers, W., Maniak, M. and Soldati, T. (1998). Ethane-freezing/methanol-fixation of cell monolayers: a procedure for improved preservation of structure and antigenicity for light and electron microscopies. *J. Struct. Biol.* **121**, 326-342.

Neuhaus, E. M., Almers, W. and Soldati, T. (2002). Morphology and dynamics of the endocytic pathway in Dictyostelium discoideum. *Mol. Biol. Cell* **13**, 1390-1407.

Pan, P., Hall, E. M. and Bonner, J. T. (1972). Folic acid as second chemotactic substance in the cellular slime moulds. *Nat. New Biol.* **237**, 181-182.

Paquet, V. E., Lessire, R., Domergue, F., Fouillen, L., Filion, G., Sedighi, A. and Charette, S. J. (2013). Lipid composition of multilamellar bodies secreted by Dictyostelium discoideum reveals their amoebal origin. *Eukaryot. Cell* **12**, 1326-1334.

Prigent, M., Dubois, T., Raposo, G., Derrien, V., Tenza, D., Rossé, C., Camonis, J. and Chavrier, P. (2003). ARF6 controls post-endocytic recycling through its downstream exocyst complex effector. *J. Cell Biol.* **163**, 1111-1121.

Ragaz, C., Pietsch, H., Urwyler, S., Tiaden, A., Weber, S. S. and Hilbi, H. (2008). The Legionella pneumophila phosphatidylinositol-4 phosphate-binding type IV substrate SidC recruits endoplasmic reticulum vesicles to a replication-permissive vacuole. *Cell. Microbiol.* **10**, 2416-2433.

Randazzo, P. A., Inoue, H. and Bharti, S. (2007). Arf GAPs as regulators of the actin cytoskeleton. *Biol. Cell* **99**, 583-600.

Rauchenberger, R., Hacker, U., Murphy, J., Niewöhner, J. and Maniak, M. (1997). Coronin and vacuolin identify consecutive stages of a late, actin-coated endocytic compartment in Dictyostelium. *Curr. Biol.* **7**, 215-218.

Ravanel, K., de Chassey, B., Cornillon, S., Benghezal, M., Zulianello, L., Gebbie, L., Letourneur, F. and Cosson, P. (2001). Membrane sorting in the

Journal of Cell Science

endocytic and phagocytic pathway of Dictyostelium discoideum. *Eur. J. Cell Biol.* **80**, 754-764.

Rivero, F. and Maniak, M. (2006). Quantitative and microscopic methods for studying the endocytic pathway. *Methods Mol. Biol.* **346**, 423-438.

Solomon, J. M., Rupper, A., Cardelli, J. A. and Isberg, R. R. (2000). Intracellular growth of Legionella pneumophila in Dictyostelium discoideum, a system for genetic analysis of host-pathogen interactions. *Infect. Immun.* **68**, 2939-2947.

TerBush, D. R., Maurice, T., Roth, D. and Novick, P. (1996). The Exocyst is a multiprotein complex required for exocytosis in Saccharomyces cerevisiae. *EMBO J.* **15**, 6483-6494.

Urwyler, S., Nyfeler, Y., Ragaz, C., Lee, H., Mueller, L. N., Aebersold, R. and Hilbi, H. (2009). Proteome analysis of Legionella vacuoles purified by magnetic immunoseparation reveals secretory and endosomal GTPases. *Traffic* **10**, 76-87.

Wallace, L. J. and Frazier, W. A. (1979). Photoaffinity labeling of cyclic-AMP- and AMP-binding proteins differentiating Dictyostelium discoideum cells. *Proc. Natl. Acad. Sci. USA* **76**, 4250-4254.

Weber, S. S., Ragaz, C., Reus, K., Nyfeler, Y. and Hilbi, H. (2006). Legionella pneumophila exploits PI(4)P to anchor secreted effector proteins to the replicative vacuole. *PLoS Pathog.* **2**, e46.

Weeks, G. G. P and Insall, R. H. (2005). The small GTPase Superfamily. In *Dictyostelium Genomics* (ed. W. F. Loomis and A. Kuspa), pp. 173-201. Far Hills, NJ: Horizon Press.

Xu, L. and Luo, Z. Q. (2013). Cell biology of infection by Legionella pneumophila. *Microbes Infect.* **15**, 157-167.